Journal of Petroleum Science and Engineering 192 (2020) 107251

Contents lists available at ScienceDirect

Journal of Petroleum Science and Engineering

journal homepage: http://www.elsevier.com/locate/petrol

Self-suspending proppant manufacturing method and its property evaluation

Weijia Cao [a], Kun Xie [a,*], Xiangguo Lu [a,**], Qing Chen [b], Zhongyuan Tian [a], Wei Lin [c]

[a] Laboratory of Enhanced Oil Recovery of Education Ministry, Northeast Petroleum University, Daqing, Heilongjiang, 163318, People's Republic of China
[b] CNPC Bohai Sea Drilling Engineering Co.,Ltd., Renqiu, Hebei, 062552, People's Republic of China
[c] University of Chinese Academy of Sciences, Beijing, 062552, People's Republic of China

ARTICLE INFO

Keywords:
Self-suspending proppant
Suspending effect
Fracture conductivity
Core damage
Field application

ABSTRACT

In recent years, a new technique involving the use of a self-suspending proppant has been a focus of research in relation to fracturing operations. The technique combines a proppant and sand-carrying fluid through the swelling and tackifying produced by the hydration material coating on the proppant surface. In this study, a self-suspending proppant was created using ceramic sand, polymer, guar gum, sucrose, and SiO_2 nanoparticles. In laboratory evaluation experiments, this self-suspending proppant showed a good suspension effect in tap water, as well as a good temperature resistance. When each 100 g of proppant had 6.6 g of HAWP powder adhering to it, and the sand ratio was greater than 10%, the self-suspending proppant was found to be completely suspended in 120 s with no settlement occurring before 200 min. Furthermore, its core damage rate was low. In a field application, self-suspending proppant fracturing was used in the M block of the H Oilfield, which is located in the southern section of Qinshui Basin, China. For the two wells in the M block, well M13-X and well M13-Y, the volumes of fracturing fluid required for construction were reduced by 334 m^3 and 351 m^3, respectively, compared with untreated proppant fracturing. In addition, the fracturing construction times were reduced by 53.4 min and 88.2 min, and the CBM production values were increased by 286 m^3 and 320 m^3, respectively. The self-suspending proppant fracturing increased the construction efficiency and CBM production, and decreased the construction difficulty and risk of overpressure. These are important research findings and show its wide applicability.

1. Introduction

Hydraulic fracturing is an important technology for increasing oil and gas production. In addition to being widely used as an effective technology in low-permeability reservoirs, it is used in the stimulation and transformation of medium- and high-permeability reservoirs (Al-Muntasheri et al., 2017; Chen et al., 2017; Li et al., 2017). During the process of hydraulic fracturing, fracturing liquids are injected into wells using high-pressure pumps, which greatly exceed the absorptive capacity of the formation, while maintaining high pressure in the wellbore (Shen et al., 2019). When the well wall tensile stress produced by this pressure is greater than the tensile strength of the formation rock, fractures occur in the formation (Lin et al., 2017, 2019). The cracking is extended with the injection of a sand-carrying fluid, and the proppant in this sand-carrying fluid is pushed into the fractures. With the continuous injection of the sand-carrying fluid, the fractures are further extended, leaving the proppant behind. After this fracture construction, the proppant prevents the fracture from completely closing. Thus, a fluid flow channel with a larger oil release area and higher conductivity is formed in the formation, which ultimately achieves the goal of increasing the production and injection (Blyton et al., 2018; Pangilinan et al., 2016; Roostaei et al., 2018). The principle behind these increases in the production and injection is decreasing the fluid seepage resistance in the formation. In other words, the goal is to change the original radial flow into a one-way flow between the reservoir and fracture and between the fracture and wellbore, which greatly reduces the energy consumption (Sun and Schechter, 2017; Wang et al., 2016; Weijermars et al., 2018). In recent years, the construction of complex and difficult wells has increased with oilfield development, simplified fracturing construction procedures, and improved fracturing efficiency, as those

* Corresponding author.
** Corresponding author.
E-mail address: 138002020222@stu.nepu.edu.cn (W. Cao).

https://doi.org/10.1016/j.petrol.2020.107251
Received 3 October 2019; Received in revised form 14 February 2020; Accepted 30 March 2020
Available online 2 April 2020

topics have been given more attention by engineers (Fang et al., 2019). The development of a fracturing system mainly includes the following tasks (Zhang et al., 2017b): (1) develop new kinds of treatments and technologies to utilize low molecular weight guar gum and reflux, or synthesize new alternatives such as other plant products or synthetic chemical fracturing fluids; (2) improve the adaptability of the fracturing fluid to high-salinity water and ensure the implementation of large-scale and industrial operations; (3) reduce the interaction with additive agents and realize he online continuous mixing of fracturing liquids; and (4) improve the proppant suspension performance and reduce costs.

Self-suspending proppant is a new type of proppant composed of a proppant and polymer hydration materials. These materials are adhered to the surface of the proppant by adhesives, and they dissolve quickly, suspending the proppant in water. Self-suspending proppants can be categorized into two types: one that involves an increase in the proppant volume by the expansion of the material adhered to the surface of the proppant and one that involves an increase in the liquid viscosity. Self-suspending proppant can be used to prepare a fracturing fluid online, which greatly reduces the cost of fracturing fluid preparation and transportation (Goldstein and VanZeeland, 2015; Kincaid et al., 2013; , Zhang et al., 2017a). In addition, based on parameters such as the injection pressure and injection speed during fracturing construction, the construction scale can be adjusted over time, which reduces the construction risk. Compared with untreated proppant (e.g., quartz sand, ceramic sand, or steel balls), the main advantages of self-suspending proppant are as follows.

(1) The polymer on the outer layer of the proppant can be quickly hydrated by water. Thus, a self-suspending proppant can be prepared online, which reduces the preparation and transportation of fracturing fluid equipment, and decreases the production and operation risk.
(2) The polymer can adhere to the surface of the proppant for a long time under high-shear action, which ensures the long-distance migration of the proppant from the wellbore to the fracture.

At present, proppant surface modification is widely used in the preparation of a self-suspending proppant. There are two main modification methods. One is to change the wettability of the proppant particles using chemical agents. In other words, hydrophobic surfactants are used to cover the surface of the proppant, which can attract gas bubbles around it and reduce the relative density, enhancing its suspension ability in water (Zhang et al., 2017b). The other method is to apply a coupling agent to the surface of the proppant and then add a series of chemical agents to synthesize a polymer onto it (Liang et al., 2018; Mou, 2017). In addition to being technologically complicated and high in cost, these preparation methods produce proppants with weak suspension ability and poor adaptability. Therefore, it is urgent to develop an efficient and low-cost preparation method for a self-suspending proppant.

This paper presents a simple and low-cost method for fabricating a self-suspending proppant. The suspension property, gel-breaking property, and fracture conductivity of a self-suspending proppant produced using this method were investigated, and the loss property and core damage of the polymer materials on the outer layer were studied. The results provide theoretical and technical support for the development of a self-suspending proppant and its application in wells.

2. Experimental procedures

2.1. Preparation process for self-suspending proppant

The self-suspending proppant was developed using ceramic sand (30 mesh), hydrophobically associating water-soluble polymer (HAWP, with the structural unit shown in Fig. 1), guar gum, sucrose, and SiO_2 nanoparticles. Among these, the polymer and guar gum were used as thickeners (Liu et al., 2017). Sucrose was used as a binder between the ceramic sand and the thickener, and the SiO_2 nanoparticles were used as a dispersant (Zhou et al., 2019). The preparation process for the self-suspending proppant was as follows.

(1) A sucrose solution with a concentration of 10 wt% was prepared using water.
(2) Ceramic sand was soaked in this sucrose solution after washing.
(3) The ceramic sand was filtered from the sucrose solution and dried, but it was necessary to keep the surface of the proppant moist.
(4) The ceramic sand, HAWP (or guar gum), and SiO_2 nanoparticles were mixed in a blender with certain proportions, and then dried to obtain many multi-particle adherent blocks.
(5) These blocks were dispersed and sifted using a roller.
(6) The particles and dust were screened after preparation, and finally, the self-suspending proppant was obtained.

The schematic diagram and steps for this operation are shown in Figs. 2 and 3, respectively.

2.2. Suspension of self-suspending proppant

The self-suspending proppant was prepared according to the above procedure, and 6.6 g of HAWP powder was adhered to each 100 g of ceramic sand. Then, the self-suspending proppant was suspended using tap water, which had a salinity of 774.9 mg/L. Sand ratios of 10%, 20%, 30%, and 40% were used, and a glass bar was used for clockwise mixing. The time required for all of the proppant to be fully suspended was recorded. Then, the solution was placed into a thermostatically controlled oven and kept at 45 °C, and the settling time was recorded after all the proppant was completely settled.

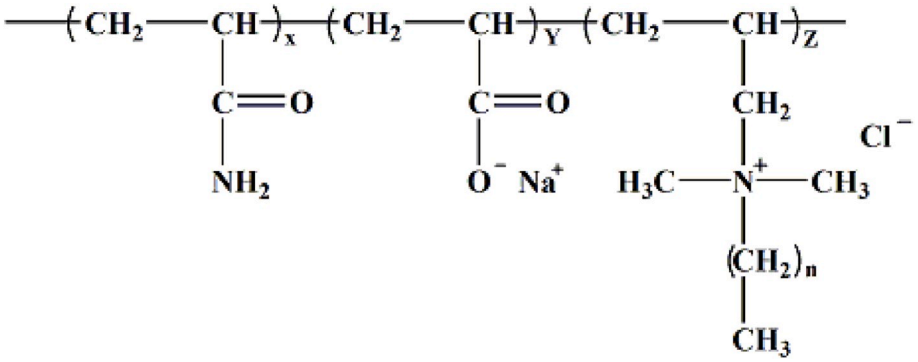

Fig. 1. Structural unit of HAWP.

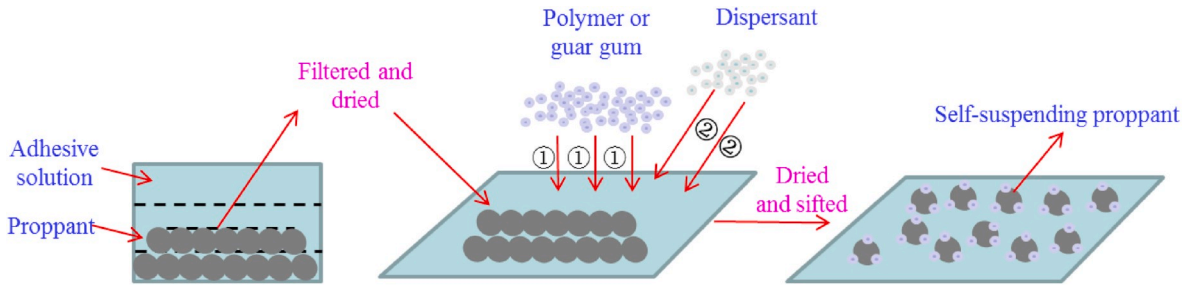

Fig. 2. Operation schematic diagram.

Fig. 3. Practical operation steps.

2.3. Fracture conductivity of self-suspending proppant

The experimental device for evaluating the fracture flow conductivity was a diversion chamber, which had a width of 4.12 cm and a length between the two pressure measurement points of 12.75 cm. Its structure is shown in Fig. 4. A pressure tester (seen in Fig. 5) was used to determine the fracture closure pressure. In addition, the experimental device also included an intermediate container, an advection pump, an electronic balance, a precision pressure gauge, and other components. The following experimental steps were used to determine the fracture conductivity.

(1) The clamp was assembled. The pipeline and joint were cleaned, and the proppant and self-suspending proppant were screened with a 30/50 mesh for the experiment.
(2) The self-suspending proppant, ceramic sand, or a mixture was weighed according to the sand concentration ($C = 2.5$ kg/m^2). It was then used to fill the diversion chamber, and the piston was covered after paving. When the fracture conductivity of the self-suspending proppant solution or ceramic sand in the fracturing fluid was tested, a gel breaker was first added to the solution, followed by a 6 h waiting period before the experiment.
(3) The chamber was pressurized to the designated closure pressures of 6.9 MPa, 10 MPa, 20 MPa, 35 MPa, 50 MPa, 65 MPa, 80 MPa,

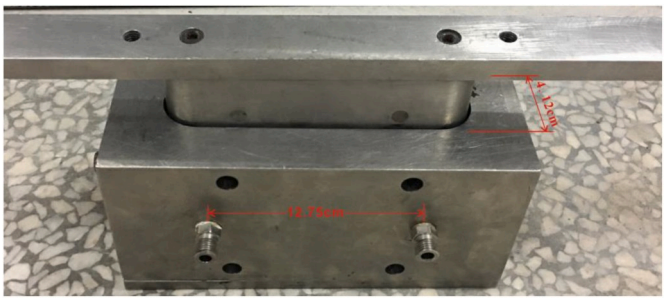

Fig. 4. Photograph of diversion chamber.

Fig. 5. Photograph of pressure testing machine.

and 90 MPa. After waiting for 15 min at each pressure point, the advection pump was opened, and the pressures at "pressure measuring point 1″ and "pressure measuring point 2″ were measured until the pressure was stable. The displacement capacity was 2 mL/min.

(4) The pump was stopped and increased to the next level of closure pressure, and step (3) was repeated until the end of the experiment.
(5) The pump was closed; the pressure of the diversion chamber was released; the pipeline was cleaned; and the power supply was turned off.
(6) The fracture conductivity and thickness of the proppant filling layer without the closure pressure were calculated using Eqs. (1) and (2) according to the Petroleum and Natural Gas Industry Standard of the Republic of China (SY/T6302-2009-2009, 2010).

$$kW_f = \frac{99.998\mu \cdot Q \cdot L}{W \cdot \Delta P} \quad (1)$$

$$W_f = \frac{0.100C}{\rho} \quad (2)$$

As the closure pressure of the diversion chamber gradually increased, the thickness of the proppant filling layer changed. The thickness values under different closure pressures were finally obtained according to the displacement between the piston and main gap after pressurization.

$$\eta = \frac{m_c}{m_p} \times 100\% \quad (3)$$

The proppant was screened after the fracture conductivity test using a 30/50 screen mesh, and the fragmentation rate was calculated according to Eq. (3).

2.4. Fracturing fluid loss property and its core damage characteristic

The fracturing fluid loss property was determined based on the Petroleum and Natural Gas Industry Standard of the Republic of China (SY/T6302-2009-2009, 2010). Artificial column cores (seen in Fig. 6) were used in the fracturing fluid loss property experiments. These cores were made up of quartz sand cemented with epoxy resin with permeabilities (k_g) of 0.05 μm^2, 0.2 μm^2, and 0.5 μm^2 (Cao et al., 2019; Li et al., 2019; Xie et al., 2016, 2018, 2019). The diameter of each core was 2.5 cm, and the length was 9.8 cm. Fig. 7 shows a schematic diagram that includes an advection pump, a pressure sensor, a core holder, a hand pump, and a middle container. With the exception of the advection pump and hand pump, all of the equipments were placed in a thermostatically controlled oven at 45 °C. The pumps was kept at room temperature. The following experimental steps were used to determine the fracturing fluid loss property.

(1) A dried core was weighed before and after being saturated with water at 25 °C. The pore volume (PV) and porosity were calculated based on the weight difference.
(2) The permeability was measured before core damage. The core was placed in a core handler, and the experiment water was injected into the core until the pressure difference was stable, at rates of 0.5 mL/min, 1 mL/min, and 1.5 mL/min. The stabilization time was not less than 30 min. Finally, the permeability was calculated.
(3) Core damage occurred. A gel breaker was added to the HAWP or self-suspending proppant solution, and the solution was placed in the thermostatically controlled oven at 45 °C for 6 h, 12 h, and 24

Fig. 6. Structure of cores.

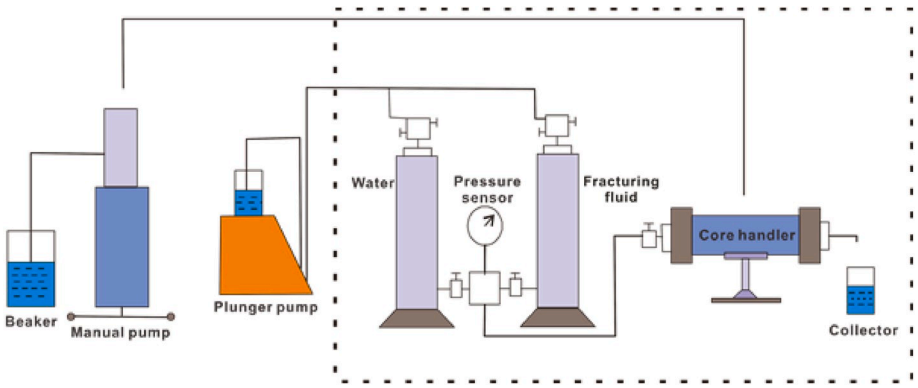

Fig. 7. Experimental process diagram.

h. Then, the solution was injected into the core, and the volume lost over a span of 3 min was recorded.

(4) The permeability after the core damage was measured. The experiment water was injected into the core until the pressure was stable, and the stabilization time was not less than 30 min. Finally, the permeability was calculated.

The core damage rate could be calculated according to Eq. (4).

$$\eta_d = \frac{k_1 - k_2}{k_1} \times 100\% \quad (4)$$

3. Analysis of experimental results

3.1. Adhesive solution

The adhesive solution should have a good stickiness at first and then have no effect on the polymer on the self-suspending proppant surface. The author found that sucrose was a good adhesive.

Sucrose exhibited strong hydrophilicity owing to its polyhydroxyl structure, whereas the hydroxyl group had a strong ability to bind to water and form a large number of hydrogen bonds. Thus, it felt sticky, which was actually the pull of the hydrogen bonds. Therefore, sucrose, through its stickiness, could bind the proppant to the polymer (shown in Fig. 8). In addition, sucrose is an organic substance and had little effect on the viscosity of the polymer. Fig. 9 shows the relationship between the polymer's viscosity and sucrose concentration. As Fig. 9 shows, when the polymer viscosity was high, the sucrose had almost no effect on it. When the polymer viscosity was low, it showed the trend of "first decreasing, then increasing, and finally decreasing" with an increase in the sucrose concentration. However, the changes were small. Therefore, the sucrose had little effect on the viscosity of the polymer solution.

Using a 30/50-mesh screen, 100 g of the self-suspending proppant was screened at room temperature several days after its preparation, and the quality of the HAWP powder that dropped from the proppant was weighted, with the results over time displayed in Table 1. According to the table, there was almost no change over time, indicating that the self-suspending proppant had good stability. In addition, the adhesive (sucrose) provided a good bond between the proppant and HAWP powder.

3.2. Suspension effect of self-suspending proppant

The suspension time and settling time of the self-suspending proppant at 45 °C are listed in Table 2. As shown, the suspension time of the proppant was shortened, whereas the settling time was prolonged and the self-suspension ability was enhanced with an increase in the sand ratio. When the sand ratio was greater than 10%, the self-suspending proppant was fully suspended in 2 min with no settlement occurring within 200 min. Therefore, it could be concluded that the self-suspending proppant exhibited a better suspension performance (seen in Fig. 10).

3.3. Gel-breaking performance of self-suspending proppant

After a fracturing operation, the high-viscosity fracturing fluid must quickly and completely break up and return to the surface. Thus, it is necessary to add a breaker to the fracturing fluid. Ammonium persulfate is usually used as a breaker. It can degrade or destroy the molecular chain of a polymer under certain temperature and pressure conditions. Then, its viscosity quickly decreases. Thus, the gel-breaking performance of a self-suspending proppant plays an important role in fracturing.

Different concentrations of ammonium persulfate microcapsules were added to solutions of the self-suspending proppant suspended in tap water using sand ratios of 10%, 20%, 30%, and 40%. The gel-breaking times at 45 °C is listed in Table 3, which shows that for sand ratios of 10% and 20%, the gel-breaking time decreased as the ammonium persulfate microcapsule concentration increased. However, for sand ratios of 30% and 40%, even when the ammonium persulfate microcapsule concentration was greater than 1%, the self-suspending proppant solution could not achieve gel-breaking, except when using a sand ratio of 30% and gel breaker concentration of 2%. This was mainly

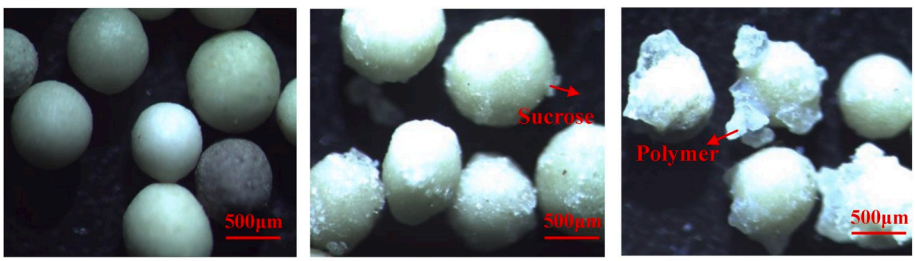

Fig. 8. (a) Picture of ceramic sand, (b) picture of ceramic sand with sucrose, and (c) picture of self-suspending proppant.

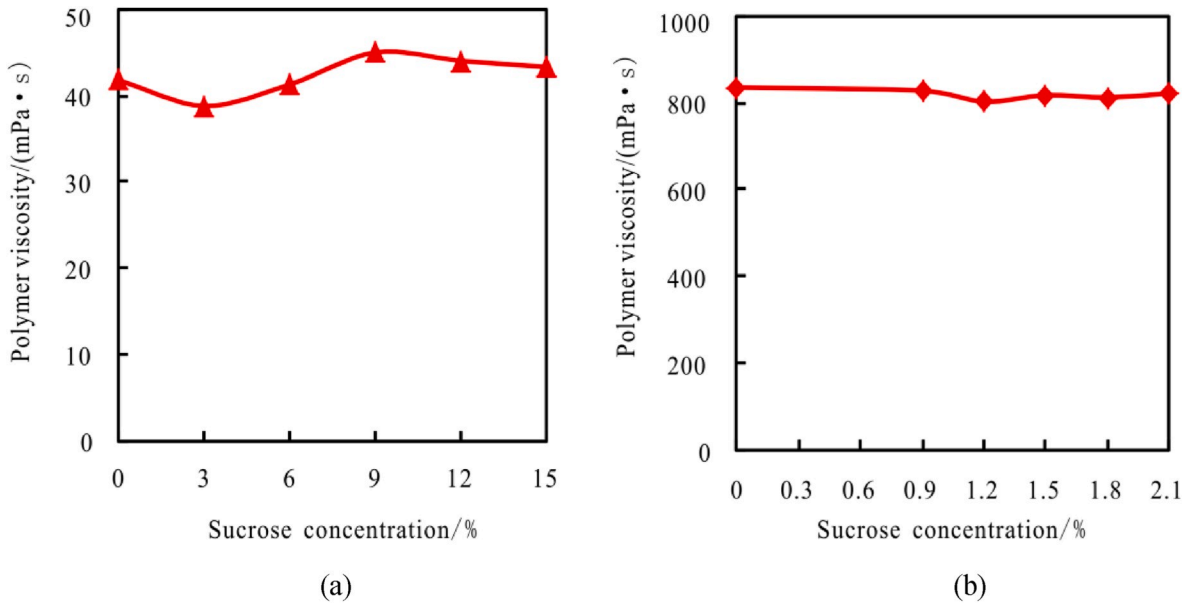

Fig. 9. Relationship between polymer viscosity and sucrose concentration: (a) C_p = 1000 mg/L (prepared using water with high salinity) and (b) C_p = 1000 mg/L (prepared using water with low salinity).

Table 1
Quality of HAWP powder that dropped from self-suspending proppant over time.

Time (d)	1	5	10	30	50	70	90
Quality of HAWP powder (g)	0.189 ± 0.005	0.187 ± 0.06	0.185 ± 0.03	0.186 ± 0.004	0.184 ± 0.005	0.183 ± 0.003	0.182 ± 0.004

Table 2
Suspension time and settling time of self-suspending proppant.

Parameter	Sand ratio (%)			
	10	20	30	40
Suspension time (s)	77	61	52	38
Settling time (min)	456	1155	>1200	>1200

because the concentration of the fracturing liquid formed by the self-suspending proppant with a sand ratio of 40% was approximately twice that with a sand ratio of 20%, and the ammonium persulfate could not break the gel in the range of experimental concentrations under a temperature of 45 °C. Thus, there was a problem. If the sand ratio was relatively high, the gel-breaking effect of the self-suspending proppant solution was poor, which affected the fracturing operation and increased the fracturing costs. This could be solved in three ways. First, the quality of the polymer powder bonded with the proppant could be changed. Second, the type of polymer powder bonded to the proppant could be changed. Finally, the untreated proppant (ceramic sand) and self-suspending proppant could be mixed in certain proportions. This third method was selected to perform the experiment. The self-suspending proppant and ceramic sand were mixed at a 1:1 ratio. Then, the mixture was suspended using tap water, with sand ratios of 10%, 20%, 30%, and 40%, and different concentrations of ammonium persulfate microcapsules were added to the fracturing fluid produced with the mixed proppant. The gel-breaking time of the mixture at 45 °C is listed in Table 4, which shows that for sand ratios of 10–40%, the solution could

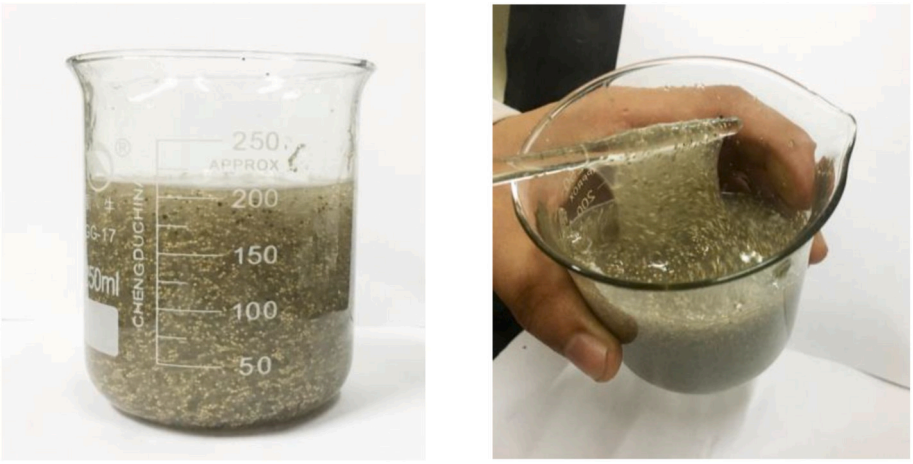

Fig. 10. Suspension performance of self-suspending proppant.

Table 3
Gel-breaking time of fracturing fluid produced using self-suspending proppant (min).

Sand ratio (%)	Ammonium persulfate microcapsules concentration (%)			
	0.3	0.5	1	2
10	268	235	165	109
20	352	319	254	164
30	No gel breaking	No gel breaking	No gel breaking	325
40	No gel breaking	No gel breaking	No gel breaking	No gel breaking

Table 4
Gel-breaking time of fracturing fluid produced using mixed proppant (min).

Sand ratio (%)	Ammonium persulfate microcapsules concentration (%)			
	0.3	0.5	1	2
10	199	172	142	105
20	282	251	183	132
30	317	286	219	147
40	371	332	271	178

achieve gel-breaking, and the time decreased as the ammonium persulfate microcapsule concentration increased. When the self-suspending proppant and ceramic sand were mixed at a 1:1 ratio, the gel-breaking time of the solution with the sand ratio of 40% was slighter longer than that of the self-suspending proppant solution with the sand ratio of 20%. An analysis showed that the volume of the ceramic sand was smaller than that of the self-suspending proppant. Thus, when the sand ratio was 40%, the content of self-suspending proppant in the mixture was greater than 50%. Thus, the concentration of polymer fracturing fluid was high, and the gel-breaking time was long.

3.4. Suspension effect of self-suspending proppant mixed with untreated proppant (ceramic sand)

Ceramic sand with adhered HAWP powder was used as the self-suspending proppant, where 6.6 g of HAWP powder was adhered to 100 g of ceramic sand. The self-suspending proppant and untreated proppant (ceramic sand) were mixed at a certain ratio. Then, the mixture was suspended using tap water, with sand ratios of 10%, 20%, 30%, and 40%. The mixture was then placed in a thermostatically controlled oven at 45 °C after achieving full suspension. The suspension time and settling time of the self-suspending proppant are shown in Fig. 11. As can be seen, when the ratio of self-suspending proppant to ceramic sand was high, the concentration of the polymer fracturing liquid increased. Thus, the suspension time of the proppant was

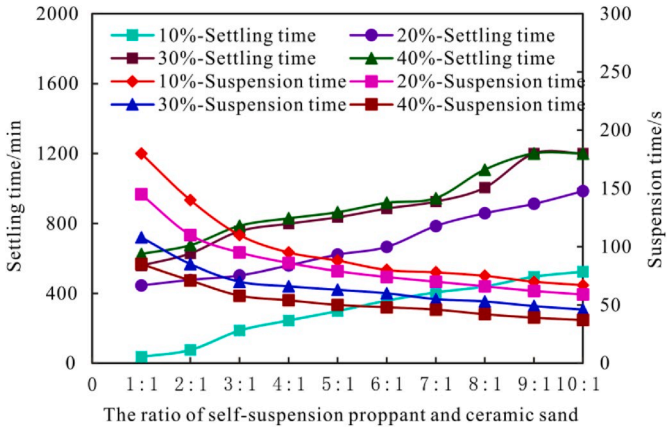

Fig. 11. Suspension time and settling time of mixtures.

shortened, the settling time was prolonged, and the self-suspending ability was enhanced. Similarly, a larger sand ratio led to a shorter suspension time for the proppant. When the self-suspending proppant was mixed with ceramic sand, the self-suspension ability decreased. However, this mixture could be more suitable for field fracturing. In addition, in the process of preparing the self-suspending proppant, a self-suspending proppant with greater polymer adhesion could first be made and mixed with ceramic sand, according to the actual fracturing construction needs. This method would not only provide great production cost savings but also improve the reservoir adaptability of the self-suspending proppant.

3.5. Suspension effect at high temperature

The self-suspending proppant with HAWP powder could not be suspended in a high-temperature reservoir. Thus, guar gum was adhered to the surface of the proppant using the preparation process discussed in the experimental procedures. For each 100 g of ceramic sand, 6.6 g of guar gum was adhered. The self-suspending proppant was placed into tap water and an organic boron crosslinker was added at a concentration of 0.6%. Then, a glass bar was used for clockwise mixing, and the suspension time and settling time were recorded at 80 °C and 150 °C. The suspension time and settling time of the self-suspending proppant are listed in Table 5, which shows that when the temperature was 80 °C and the sand ratio was 30%, suspension could be achieved in several seconds, with no settlement occurring within the first 200 min. When the temperature was increased to 150 °C, the suspension time increased and the settling time decreased. Generally, the guar gum adhered to the self-suspending proppant maintained good heat resistance.

3.6. Fracture conductivity of self-suspending proppant

The viscosity of the outer hydration material greatly increased after the self-suspending proppant came into contact with water. It soon became a mixture of ceramic sand and fracturing fluid. To study the effect of the outer hydration material on the ceramic sand during preparation, tests were conducted to determine the fracture conductivities of the self-suspending proppant in water, ceramic sand in water, ceramic sand in the fracturing fluid, and a mixture of the self-suspending proppant and ceramic sand in water based on the previously mentioned experimental procedures. To measure the fracture conductivity of the self-suspending proppant in water or ceramic sand in the fracturing fluid, a gel breaker was first added to the solution, followed by a 6 h waiting period before the experiment. The experiment results are shown in Fig. 12. As can be seen in Fig. 12, the fracture conductivity first rapidly decreased and then slowly decreased with the fracture closure pressure. It could be explained that when the closure pressure began to increase, the flowing section of the pore decreased, and the core permeability greatly decreased, causing a rapid decrease in the fracture conductivity. When the closure pressure reached 60 MPa, the proppant began to break. Because the proppant and crushed particles had a high degree of compaction, even though the closure pressure continued to increase, the fracture conductivity slowly decreased, and the curve

Table 5
Suspension time and settling time of self-suspending proppant at high temperature.

Sand ratio (%)	Temperature			
	80 °C		150 °C	
	Suspension time (s)	Settling time (min)	Suspension time (s)	Settling time (min)
10	55	56	77	36
20	41	109	55	85
30	24	277	39	254
40	13	384	25	334

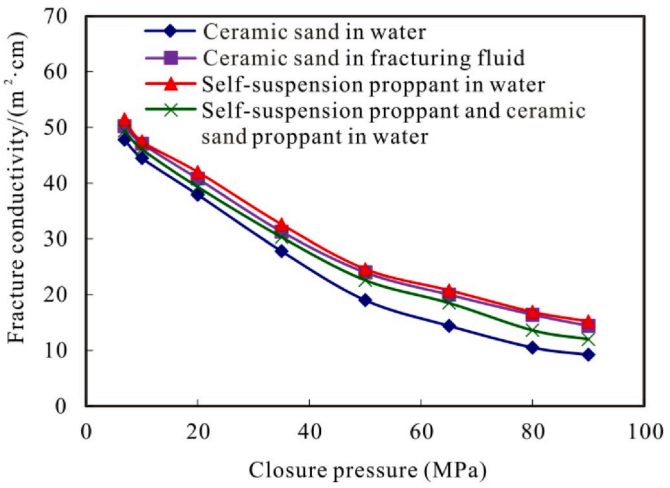

Fig. 12. Relationship between fracture conductivity and closing pressure.

tended to be stable.

It was found that the fracture conductivity of the ceramic sand in the fracturing fluid was larger than that of the ceramic sand in water, which indicated that the fracturing fluid could enhance the compressive resistance of the proppant, decrease its fragmentation rate (as seen in Table 6), and increase the fracture conductivity. However, at times, the retention of the fracturing fluid in pores led to an increase in the seepage resistance, which would decrease the fracture conductivity. Thus, when the effect of the former in improving the fracture conductivity was greater than that of the latter, the fracture conductivity increased, and vice versa. To test whether the performance of polymer (HAWP) was affected by the preparation process of self-suspension proppant, we prepared HAWP solution that had the same concentration as the self-suspension proppant solution with a sand concentration of 20%. The concentration could be calculated according to the proportion of polymer powder and ceramic in the preparation process and sand ratio. Fracturing fluid loss property experiments were carried out as experimental procedures, with core damage results shown in Table 7. It could be seen that the fracturing fluid did great damage to the core with low permeability, and the damage rate decreased with the prolongation of gel-breaking time. With the addition of gel breaker in the fracturing fluid for 12 h, the damage rate decreased greatly. When the fracturing fluid was completely broken, the damage rate was the lowest. The core damage of self-suspension proppant solution was also found to be a little lower than that of the HAWP solution with same concentration, which indicated that the performance of polymer on the surface of self-suspension proppant had not changed significantly.

The fracture conductivity of the self-suspended proppant in water was slightly larger than those of the ceramic sand in the fracturing fluid and the mixture (self-suspending proppant and ceramic sand) in water. When the self-suspending proppant was mixed with water, on the one hand, the outer layer of the self-suspending proppant was rapidly dissolved and tackified, and the inner layer of the proppant was evenly dispersed in the viscous liquid. On the other hand, because water is a low viscosity phase fluid, the dissolution mode greatly improved the dispersion degree of the self-suspending proppant, which ensured that it had good pressure resistance. When ceramic sand was added to the fracturing fluid solution, the fracturing fluid had a high viscosity phase, and the dispersion ability of the ceramic sand decreased. Therefore, the conductivity of the self-suspending proppant in water was slightly greater than that of the proppant in the fracturing fluid.

In summary, the compressive capacity and fracture conductivity of ceramic sand in the fracturing fluid and those of the self-suspending proppant in water had little difference, and that difference could be neglected. Therefore, it can be said that the self-suspending proppant prepared by this method retained the original properties of ceramic sand very well. The use of the self-suspending proppant removed the need to prepare and transport a fracturing fluid and improved the work efficiency, which led to better technical effects.

Table 6
Fragmentation rate of proppant.

Type	Sand concentration/ (kg/m^2)	Maximum pressure/ MPa	Time/ min	Fragmentation rate/%
Ceramic sand in water	2.5	90	15	14.65
Ceramic sand in fracturing fluid				11.23
Self-suspension proppant in water				12.05
Self-suspension proppant and ceramic sand in water				12.88

3.7. Field application

The M block of the H oilfield is located in the southern Qinshui Basin, which is presently the largest coalbed methane (CBM) production base in China. The depth of the coal seam is 550–1800 m, with 87.9% over 800 m. The thickness is stable, and the average is approximately 6 m. Self-suspending proppant was used in well M13-X and well M13-Y of the M block, and achieved good fracturing effects.

The construction and final results of the fracturing for well M13-X and well M13-Y are shown in Table 8, Figs. 13 and 14.

As can be seen from Table 8, Figs. 13 and 14, in the M block of the H oilfield, five wells carried out fracturing operations. Among them, well M13A, well M13B, and well M13C used untreated proppant for fracturing, for which the average volume of the fracturing fluid was approximately 1241 m^3, the average construction time was approximately 240 min, and the CBM production was approximately 2654 m^3. Compared with these three wells, well M13X started self-suspending proppant fracturing 134 min after the start of untreated proppant fracturing, and the operation lasted 40 min. The volume of fracturing fluid required for fracturing construction was reduced by 334 m^3, and the fracturing construction time was reduced by 53.4 min. In addition, the CBM production was increased by 286 m^3 compared with untreated proppant fracturing. Well M13Y started self-suspending proppant fracturing 142 min after the start of untreated proppant fracturing, and it saved 351 m^3 of fracturing fluid. In addition, the fracturing construction time was reduced by 88.2 min, and CBM production was increased by 320 m^3. In conclusion, self-suspending proppant fracturing enhanced the construction efficiency and decreased the construction difficulty and risk of overpressure. More importantly, it increased the CBM production and demonstrated wide applicability. Thus, it represents an important research finding.

4. Conclusion

1. Sucrose has strong hydrophilicity. It not only had a good initial stickiness but also demonstrated no effect on the polymer on the surface of the self-suspending proppant. Thus, it was a good adhesive.
2. The self-suspending proppant had good stability. Its suspension time decreased with an increase in the sand ratio, and the settling time increased.
3. For reservoir temperatures of 80 °C or 150 °C, guar gum adhered to the proppant could be suspended in several seconds, and it demonstrated no settlement within 200 min with a sand ratio of 30%.

Table 7
Core damage rate of fracturing fluid.

Fracturing fluid type	Time of gel breaker was added in fracturing fluid (h)	Permeability ($\times 10^{-3}\mu m^2$)		Cumulative loss volume (mL)	Damage rate (%)
		Before damage	After damage		
Self-suspension proppant solution	6	39.2	29.3	1.51	25.26
		128.1	100.3	2.01	21.70
		392.3	331.6	2.53	15.47
	12	41.4	32.4	1.66	21.74
		129	103.3	2.22	19.92
		407.4	346.9	2.77	14.85
	24	40.4	31.8	1.67	21.29
		134.8	108.6	2.25	19.44
		399.4	341.2	2.81	14.57
HAWP solution	6	39.5	28.9	1.26	26.84
		128.6	96.7	1.81	24.81
		398.6	326.4	2.24	18.11
	12	40.7	31.5	1.41	22.60
		131.5	104.7	1.96	20.38
		396.9	329.7	2.39	16.93
	24	41.3	32.2	1.44	22.03
		129.2	103.1	1.99	20.20
		402.2	334.4	2.43	16.86

Table 8
Construction fluid volume, construction time and CBM production in well M13-X and well M13-Y.

Well number	Construction fluid volume /m^3	Sand volume /m^3	Time /min	CBM production /m^3
M13-X	907	100	186.6	2940
M13-Y	890	100	151.8	2974
M13-A	1240.8	100	242	2543
M13-B	1241.5	100	235	2654
M13-C	1241.5	100	244	2765

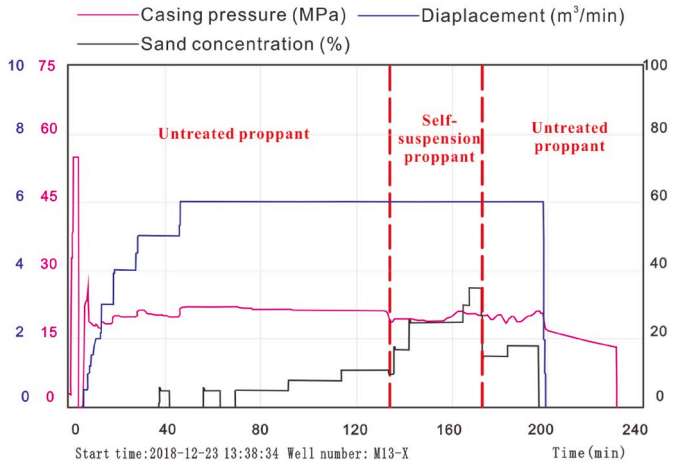

Fig. 13. Fracturing construction results when using self-suspending proppant in well M13-X.

4. A self-suspending proppant with higher polymer adhesion could first be made and then mixed with untreated proppant according to the actual fracturing construction needs, which would greatly reduce the production cost.
5. The compressive capacities and fracture conductivities of the untreated proppant in the fracturing fluid and self-suspending proppant in water were almost the same. Furthermore, the core damage after the suspension of the self-suspending proppant was slightly lower than that with a HAWP solution at the same concentration.
6. Self-suspending proppant fracturing was used in well M13-X and well M13-Y of the H Oilfield in the southern Qinshui Basin,

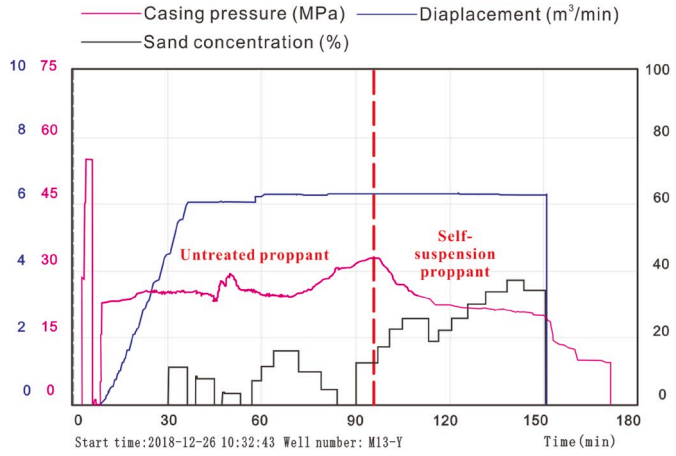

Fig. 14. Fracturing construction results when using self-suspending proppant in well M13-Y.

decreasing the fracturing fluid volume and time required for fracturing construction and increasing the CBM production. The use of the self-suspending proppant mitigated the need to prepare and transport a fracturing fluid and improved the work efficiency, which reduced the construction difficulty and risk of overpressure.

CRediT authorship contribution statement

Weijia Cao: Data curation, Formal analysis, Writing - original draft, Visualization. **Kun Xie:** Data curation, Formal analysis, Writing - original draft, Visualization. **Xiangguo Lu:** Conceptualization, Methodology, Supervision, Investigation. **Qing Chen:** Resources. **Wei Lin:** Writing - review & editing.

Acknowledgments

This work was supported by the SPE Nico van Wingen Memorial Fellowship, Natural Science Foundation of China (No. 51574086), China National Science and Technology Projects (2016 ZX05058-003-010), Postdoctoral Innovative Talents Support Program of China (BX20190065).

Appendix A. Supplementary data

Supplementary data to this article can be found online at https://doi.org/10.1016/j.petrol.2020.107251.

References

Al-Muntasheri, G., Liang, F., Hull, K., 2017. Nanoparticle-enhanced hydraulic-fracturing fluids: a review. SPE Prod. Oper. 32 (2), 186–195. https://doi.org/10.2118/185161-PA.

Blyton, C., Gala, D., Sharma, M., 2018. A study of proppant transport with fluid flow in a hydraulic fracture. SPE Drill. Complet. 33 (4), 1–17. https://doi.org/10.2118/174973-PA.

Cao, W., Xie, K., Lu, X., et al., 2019. Effect of profile-control oil-displacement agent on increasing oil recovery and its mechanism. Fuel 237, 1151–1160. https://doi.org/10.1016/j.fuel.2018.10.089.

Chen, Y., Nagaya, Y., Ishida, T., 2017. Observations of fractures induced by hydraulic fracturing in anisotropic granite. Rock Mech. Rock Eng. 48 (4), 1455–1461. https://doi.org/10.1007/s00603-015-0727-9.

Fang, Y., Yang, E., Yin, D., et al., 2019. Study on distribution characteristics of microscopic residual oil in low permeability reservoirs. J. Dispersion Sci. Technol. 1–10 https://doi.org/10.1080/01932691.2019.1594886.

Goldstein, B., VanZeeland, A., 2015. Self-suspending proppant transport technology increases stimulated reservoir volume and reduces proppant pack and formation damage. Houston. In: Presented at the SPE Annual Technical Conference and Exhibition, pp. 28–30. https://doi.org/10.2118/174867-MS. September.

Kincaid, K., Snider, P., Herring, M., et al., 2013. Self-Suspending Proppant. Presented at the SPE Hydraulic Fracturing Technology Conference, Woodlands, 4-6 February. https://doi.org/10.2118/163818-MS.

Li, J., Niu, L., Lu, X., 2019. Performance of ASP compound systems and effects on flooding efficiency. J. Petrol. Sci. Eng. 178, 1178–1193. https://doi.org/10.1016/j.petrol.2019.02.092.

Li, S., Zhang, D., Li, X., 2017. A new approach to the modeling of hydraulic-fracturing treatments in naturally fractured reservoirs. SPE J. 22 (4), 1064–1081. https://doi.org/10.2118/181828-PA.

Liang, T., Fan, Z., Guo, J., et al., 2018. Study on fluorine-free superhydrophobic CeO_2@Fabric coating for cell fluid-water separation. Basic Clin. Pharmacol. 124, 402–409.

Lin, W., Li, X., Yang, Z., et al., 2019. Multiscale digital porous rock reconstruction using template matching. Water Resour. Res. 55 (8), 6911–6922. https://doi.org/10.1029/2019WR025219.

Lin, W., Yang, Z., Li, X., et al., 2017. A method to select representative rock samples for digital core modeling. Fractals 25 (4), 1–9.

Liu, R., Pu, W., Sheng, J., et al., 2017. Star-like hydrophobically associative polyacrylamide for enhanced oil recovery: comprehensive properties in harsh reservoir conditions. J. Taiwan Inst. Chem. E. 80, 639–649. https://doi.org/10.1016/j.jtice.2017.08.043.

Mou, S., 2017. Research on Technologies of Fracturing Proppant. University of Science and Technology, Beijing, China.

Pangilinan, K., De Leon, A., Advincula, R., 2016. Polymers for proppants used in hydraulic fracturing. J. Petrol. Sci. Eng. 145, 154–160. https://doi.org/10.1016/j.petrol.2016.03.022.

Roostaei, M., Nouri, A., Fattahpour, V., et al., 2018. Numerical simulation of proppant transport in hydraulic fractures. J. Petrol. Sci. Eng. 163, 119–138. https://doi.org/10.1016/j.petro.2017.11.044.

Shen, W., Song, F., Hu, X., et al., 2019. Experimental study on flow characteristics of gas transport in micro-and nanoscale pores. Sci Rep-Uk 9, 10196. https://doi.org/10.1038/s41598-019-46430-2.

Sun, J., Schechter, D., 2017. Pressure-transient characteristics of fractured horizontal wells in uncommon shale reservoirs with construction of data-constrained discrete-fracture network. SPE Prod. Oper. 33 (1), 1–11. https://doi.org/10.2118/184060-PA.

SY/T6302-2009, 2010. Recommended Practices for Evaluating Short Term Proppant Pack Conductivity [S]. China petroleum industry press, Beijing.

Wang, D., Li, Y., Hu, Y., et al., 2016. Integrated dynamic evaluation of depletion-drive performance in naturally fractured- vuggy carbonate reservoirs using DPSO-FCM clustering. Fuel 181, 996–1010. https://doi.org/10.1016/j.fuel.2016.05.009.

Weijermars, R., Harmelen, A., Zuo, L., et al., 2018. Flow interference between hydraulic fractures. SPE Reservoir Eval. Eng. 21 (4), 942–960. https://doi.org/10.2118/194196-PA.

Xie, K., Cao, B., Lu, X., et al., 2019. Matching between the diameter of the aggregates of hydrophobically associating polymers and reservoir pore-throat size during polymer flooding in an offshore oilfield. J. Petrol. Sci. Eng. 177, 558–569. https://doi.org/10.1016/j.petrol.2019.02.076.

Xie, K., Lu, X., Li, Q., et al., 2016. Analysis of reservoir applicability of hydrophobically associating polymer. SPE J. 21 (1), 1–9. https://doi.org/10.2118/174553-PA.

Xie, K., Lu, X., Pan, H., et al., 2018. Analysis of dynamic imbibition effect of surfactant in microcracks of reservoir at high temperature and low permeability. SPE Prod. Oper. 33 (3), 596–606. https://doi.org/10.2118/189970-PA.

Zhang, J., Liu, K., Cao, M., 2017. Experimental study on modified polyacrylamide coated self-suspending proppant. Fuel 199, 185–190. https://doi.org/10.1016/j.fuel.2017.02.103.

Zhang, X., Wang, Z., Wang, L., et al., 2017. Preparation and performance evaluation of intumescent self-suspending proppant. Oilfield Chem. 24 (3), 449–455. https://doi.org/10.19346/j.cnki.1000-4092.2017.03.014.

Zhou, Y., Wu, X., Zhong, X., et al., 2019. Surfactant-augmented functional silica nanoparticle based nanofluid for enhanced oil recovery at high temperature and salinity. ACS Appl. Mater. Interfaces 11 (49), 45763–45775. https://doi.org/10.1021/acsami.9b16960.